Comparisons of FEM Approaches Modelling the Metal Plastic Behaviour

A.M. Habraken, A.F. Gerday, B. Diouf and L. Duchêne

ArGEnCo Department, MS²F Division, ULg, Chemin des Chevreuils 1, 4000 Liège, Belgium

Abstract. Simple phenomenological laws (e.g. classical Hill 1948 quadratic law) are compared to more complex laws based on crystal plasticity through various numerical simulations: mechanical tests of ECAE materials, nanoindentation of titanium alloys and copper, and large strain torsion of copper bars. Taking into consideration the complexity of the investigated processes, the numerical results present rather good agreements with experimental observations.

Keywords: Constitutive laws, crystal plasticity, ECAE materials, nanoindentation, Swift effect.
PACS: 83.60.-a

INTRODUCTION

The microscopic mechanisms involved during plastic deformation of metals are various and very complex, depending on the material, the mechanical test and the experimental conditions investigated. Nowadays, numerous complex constitutive laws are developed in order to model as accurately as possible more and more complex mechanical forming processes.

On one hand, sophisticated phenomenological models (dedicated to yield locus anisotropy or/and hardening behaviour) with an increasing number of parameters are proposed. On the other hand, the material models based on the physics include more and more refined microscopic mechanisms.

As a consequence, the numerical models must be adapted to the studied material. As an example, the mechanical tests performed on ECAE material (see below) required a particular constitutive law using a kinematic hardening with an initial back-stress. Besides, the nanoindentation presented hereafter required a material model adapted to the microscopic scale of this process. Finally, the accuracy level of the constitutive law must be related to the results that are under investigation. For instance, during the large strain torsion presented in this paper, the classical Hill 1948's law was accurate enough to correctly model the stress field. While a more complex law with deep physical roots was required when second order phenomena like the Swift effect were analysed.

CRYSTAL PLASTICITY BASED CONSTITUTIVE LAWS

For the nanoindentation tests, two constitutive laws are used. The first one is a macrosopic Von Mises EP constitutive law (not described here). The second one is a microscopic crystal plasticity-based EVP constitutive law written by Huang [1]. Based on the Schmid law, the slipping rate $\dot{\gamma}^{(\alpha)}$ of the α^{th} slip system in a rate-dependent crystalline solid is determined by the corresponding resolved shear stress $\tau^{(\alpha)}$ as

CP907, *10th ESAFORM Conference on Material Forming*, edited by E. Cueto and F. Chinesta

$$\dot{\gamma}^{(\alpha)} = \dot{a}^{(\alpha)} \left(\frac{\tau^{(\alpha)}}{g^{(\alpha)}} \right)^{m} \qquad 1$$

where $\dot{a}^{(\alpha)}$ is the reference strain rate on slip system α, $g^{(\alpha)}$ is a variable which describes the current strength of that system and m is linked to the strain rate sensitivity. The strain hardening is characterized by the evolution of $g^{(\alpha)}$:

$$\dot{g}^{(\alpha)} = \sum_{\beta} h_{\alpha\beta} \dot{\gamma}^{(\beta)} \qquad 2$$

where $h_{\alpha\beta}$ are the slip hardening moduli, the sum ranges over all activated slip systems. Here, the hardening matrix is defined by Asaro and Needleman [1].

For the large strain torsion tests, a crystal plasticity law adapted to macroscopic simulations was used. This law is based on a local yield locus approach able to predict texture evolution during FE modelling of industrial forming processes. With this model, only a small zone of the yield locus is computed. This zone is updated when its position is no longer located in the part of interest in the yield locus or when the yield locus changes due to texture evolution.

This model is specific in the sense that it does not use a yield locus formulation either for plastic criterion or in the stress integration scheme. A linear stress-strain interpolation in the 5-dimensional (5D) stress space is used at the macroscopic scale:

$$\underline{\sigma} = \tau \underline{\underline{C}} \bullet \underline{u} \qquad 3$$

In this equation, $\underline{\sigma}$ is a 5D vector containing the deviatoric part of the stress; the hydrostatic part being computed according to an isotropic elasticity law. The 5D vector $\underline{u}$ is the deviatoric plastic strain rate direction (it is a unit vector). τ is a scalar describing an isotropic work hardening.

The macroscopic anisotropic interpolation is included in matrix $\underline{\underline{C}}$. Its identification relies on 5 directions: $\underline{u_i}$ (i=1…5) advisedly chosen in the deviatoric strain rate space and their associated deviatoric stresses: $\underline{\sigma_i}$ (i=1…5) computed by the polycrystal plasticity model. This micro-macro model uses Taylor's assumption of equal macroscopic strain and microscopic crystal strain. It computes the average of the response of a set of representative crystals evaluated with a microscopic model taking into account the plasticity at the level of the slip systems. In this paper, two versions of this Full Constraints (FC) Taylor's model are investigated: one coupled with a rate insensitive crystal plastic model and one coupled with a visco-plastic crystal model.

Texture evolution is computed using Taylor's model on the basis of the strain history for each integration point every 10 FE time steps. Further details and properties of Minty law can be found in [2].

APPLICATIONS

Predicted behaviour of ultrafine grained aluminium produced by ECAE subjected to compression tests

Results of FEM simulations predicting the mechanical behaviour at room temperature of test specimen of ultrafine-grained aluminium produced by ECAE

following route B_C [3] for 8 passes, are presented. The constitutive law was either based on a Hill model or on the Minty micro-macro model and coupled with an isotropic hardening law and/or kinematic hardening law.

The reference axes are defined in Figure 1a. The compression axis of the sample was aligned with the ECAE Extrusion Direction. The deformed samples at 40% and 80% of uniaxial strain were optically measured and in Figure 1b the thick lines correspond to the actual cutting of the sample. The outer lines correspond to the (possible) test specimen edges. The middle line corresponds to the position of the horizontal midplane. FE simulations were used to compare the final predicted and experimental sample shapes after compression tests. Two yield loci, coupled with the isotropic Voce model and with the constant back stress already identified in a previous paper [3], were applied to these simulations: Hill 1948 and Minty micro-macro model.

The Coulomb model was used to model the contact and a friction coefficient of 0.1 allowed predicting the measured barreling effect. Three dimensions mixed type elements [4] were used; half of the test specimen was meshed as no other symmetry than the horizontal midplane was assumed. Figure 2 compares the predicted and measured midplane sections on 40% and 80% deformation. As the Hill yield locus was identified with the hypothesis that the Transversal and the Normal Directions were orthotropic axes, the Hill simulation predicted an elliptic shape in those directions. The Minty yield locus was also identified in these axes but none symmetry was assumed. Its shape is clearly close to the actual yield locus of the ECAE material as it predicted both the elliptic shape and its rotation during the compression. Note that the Minty law did not take into account the texture evolution during the compression; it just used the initial texture to define an accurate initial anisotropic yield locus.

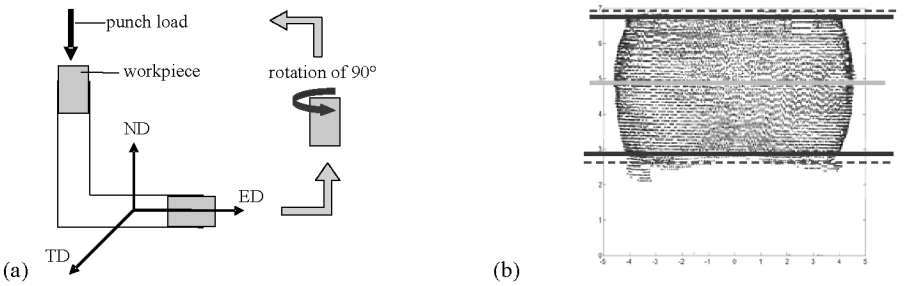

FIGURE 1. (a) ECAE process route B_C and (b) profile measurement on a sample compressed until 80% (Initial specimen geometry: 9 mm height, 6 mm diameter).

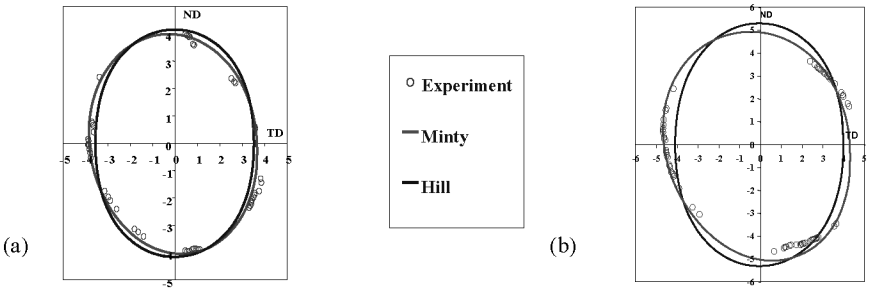

FIGURE 2. Midplane measurement and simulation for compression on 40% (a) and 80% (b).

The Minty micro-macro model coupled with a Voce type hardening model gave a good agreement with experimental results for the prediction of the shape at different stages of deformation of a compressed test specimen.

Nanoindentation

Nanoindentation is an important and versatile tool for measuring the mechanical properties of materials at micro- and nanometer length scale [5-6]. It allows obtaining the mechanical properties of a particular phase of a material by inverse modelling. Here is presented the influence of different parameters on the results in the nanoindentation simulations. First, an EP constitutive law with a three-sided diamond Berkovich indenter and a 1772 elements [7] mesh were used to model the behaviour of the β-phase of a new generation of Ti-alloy, named Ti-555 (Ti-5Al-5Mo-5V-3Cr-0.3Fe). With this law, changes of the elastic modulus and the plastic strengh (Figure 3) had a great influence on the force-displacement results. Other parameters like friction coefficient, tangent modulus or Poisson's ratio led to very small deviations.

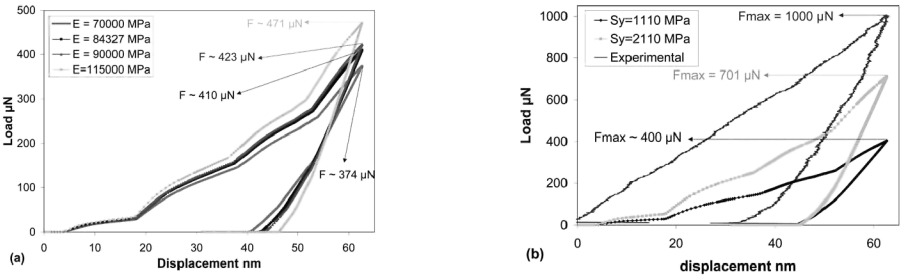

FIGURE 3. Nanoindentation tests on Ti-555. Experimental results and numerical results with different values of (a) the elastic modulus and (b) the plastic strength.

As shown in Figure 4, the geometry of the tip had to be modelled accurately. Small geometrical modifications in the definition of the indenter led to noticeable changes in the force-displacement curves.

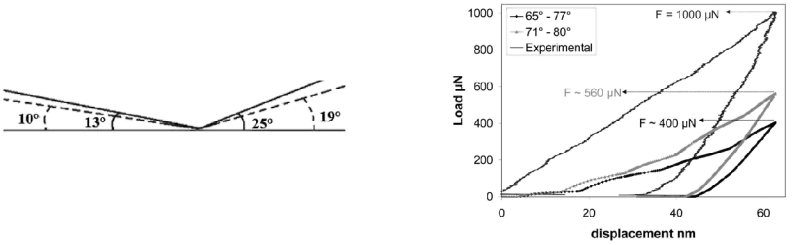

FIGURE 4. Nanoindentation test on Ti-555. Experimental and numerical results with different values the magnitude angle.

The results obtained for copper (The parameters used come from [1] and the mesh used contains 4480 elements [7]) whith different orientations of the indented grain using the microscopic law of Huang and Kysar are presented hereafter. The influence of the orientation of the crystal indented was expected, as shown in Figure 5 for

copper. Here, a conical tip was used to avoid symmetries other than those of the crystal structure. Near the indented zone, the surface of the material presented different profiles and symmetry according to the crystal orientation after an indentation depth of 125 nm. These results are similar to the literature [8].

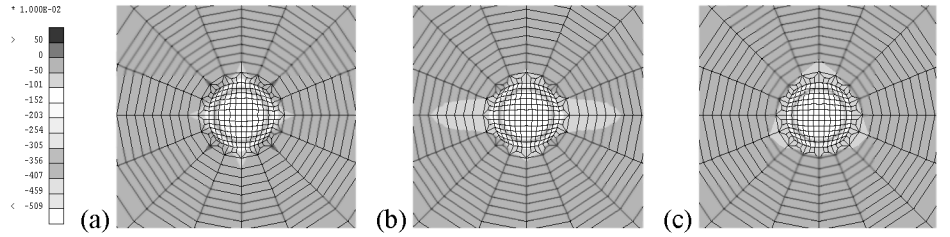

FIGURE 5. Variation depth profile of the indented surface of the material for 3 orientations of the crystal. In the global axes, the directions (100) and (001) become, (a) (100) and (001), (b) (100) and (011) and (c) (10-1) and (111), with indentation along the (001) direction in the global axes.

Swift effect prediction

The free-end torsion of copper bars was simulated with different constitutive laws: the phenomenological Hill's law and the micro-macro Minty law with and without computation of the texture evolution coupled with the elasto-plastic and elasto-visco-plastic Taylor's model. Due to the large strains involved in this torsion process, a remeshing technique dedicated to torsion simulations was applied. Further details about experimental procedure can be found in [9] while the numerical simulations are described in [10] and [11].

The axial lengthening of the cylinder induced by the torsion, i.e. the so-called Swift effect, is analysed. The axial lengthening as a function of the shear strain is plotted in Figure 6. It appears that when Hill's law and Minty law without computation of the texture evolution were used, no lengthening was obtained.

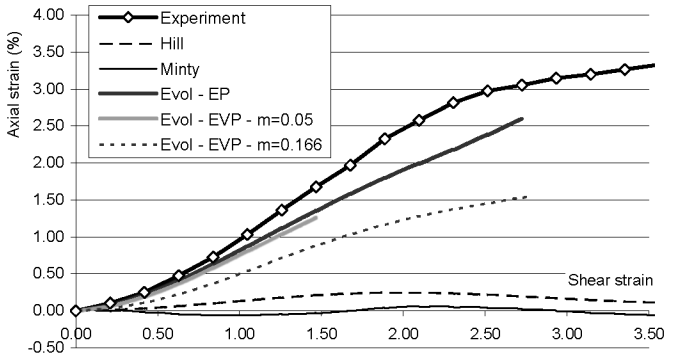

FIGURE 6. Axial lengthening versus shear strain during free end torsion of copper bars. 'Minty' refers to the law Minty without texture updating; 'Evol' refers to that law with texture evolution; 'EP' means elasto-plastic; 'EVP' is elasto-visco-plastic for which the value of the strain rate sensitivity parameter m is indicated.

The results obtained with Minty law with the elasto-plastic microscopic model and computation of the texture evolution were in rather good agreement with experimental results. As expected, the results with the elasto-visco-plastic model with a very low strain rate sensitivity value (m=0.05) were very close to the results of the elasto-plastic model. When a larger m value was employed, the predicted lengthening was too low.

It can be concluded that, for the Swift effect modelling, an accurate crystal plasticity constitutive law is required; the computation of the texture evolution must be activated. A significant influence of the strain rate sensitivity parameter was observed.

CONCLUSIONS

The choice of an adequate constitutive law as a function of the studied material, the process and the analysed results is a very important point. Unfortunately, it is not straightforward. A compromise must be done between the desired accuracy and the maximum acceptable computation time, bearing in mind that a good understanding of the underlying microscopic events is a crucial point for an efficient modelling.

For the three presented applications, satisfactory results were obtained with, for each case, a well adapted constitutive law. For the studied laws, accurate material parameters were required (especially difficult to obtain for complex laws). An efficient identification method coupled with well selected experimental tests had to be defined.

Beside an accurate constitutive law, an efficient FE formulation (including the kinematics of the element) and adequate boundary conditions were also very important points.

ACKNOWLEDGMENTS

The authors thank the Belgian Federal Science Policy Office (Contract P5/08) for their financial support. As Research Director, A.M. Habraken thanks the Fund for Scientific Research (FNRS, Belgium) for its support.

REFERENCES

1. Y. Huang, "A user-material subroutine incorporating single crystal plasticity in the ABAQUS finite element program", Internal report, 2005.
2. A.M. Habraken and L. Duchêne, *Int. J. of Plasticity* **20**, 1525-1560 (2004).
3. S. Poortmans, F. El Houdaigui, A. Habraken, B. Verlinden, in "Untrafine Grained Materials IV", in *Proc. TMS-Conference 2006*, edited by Y.T. Zhu et al., 389-394.
4. Y. Zhu, S. Cescotto, *Comp. Meth. in Applied Mechanics and Engineering*, 129, 177–209, 1995.
5. R.Saha and W.D.Nix, *Acta Materialia*, 50 (2002) 23-38.
6. P.L.Larsson, A.E.Giannakopoulos, E.Söderlung, D.J.Rowcliffe, R.Vestergaard, *Int. J. Solids Structures*, Vol.33, No.2, pp.221-248, 1996.
7. A.F.Gerday,N.Clement, P.J.Jacques, T.Pardoen, A.M.Habraken, "FE simulations of nanoindentation in beta metastable Ti", in *Proc. ESAFORM 2006*, edited by N. Juster and A. Rosochowski, Poland.
8. Y. Wang, D.Raabe, C.Klüber, *Acta Materialia* **52**, 2229-2238 (2004).
9. L.S. Toth, J.J. Jonas, D. Daniel and J.A. Bailey, *Textures and Microstructures* **19**, 245-262 (1992).
10. L. Duchêne, F. El Houdaigui and A.M. Habraken, "Finite element simulations of the Swift effect" in *Proc. ICTP 2005*, edited by P.F. Bariani, Padova.
11. L. Duchêne, F. El Houdaigui, A.M. Habraken, "Length changes and texture prediction during free end torsion test of copper bars with FEM and remeshing techniques", *Int. J. of Plasticity*, to appear.